Dergi Listesi

Dergi Adı

ISSN 1369-8001

Yıl 2021

Temizle | Ara

No	Yıl	Dergi Adı	ISSN	Çeyreklik Grup	Katsayı	kategori	Dergi Puanı
99608	2021	MATERIALS SCIENCE IN SEMICONDUCTOR PROCESSING	1369-8001	Q1	1	SCIE	

Sayfada 10 Kayıt Göster

Önceki 1 Sonraki

1 Kayıttan 1 - 1 Arası Kayıtlar

Materials Science in Semiconductor Processing 140 (2022) 106411

Contents lists available at ScienceDirect

Materials Science in Semiconductor Processing

journal homepage: www.elsevier.com/locate/mssp

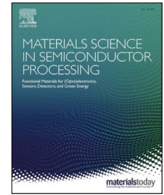

Theoretical analyses of the carrier localization effect on the photoluminescence of In-rich InGaAs layer grown on InP

Marwa Ben Arbia [a,*], Badreddine Smiri [a,d], Ilkay Demir [b], Faouzi Saidi [a,c], Ismail Altuntas [b], Fredj Hassen [a], Hassen Maaref [a]

[a] Laboratoire de Micro-optoélectronique et Nanostructures (LR99ES29), Université de Monastir, Faculté des Sciences Monastir, Avenue de l'Environnement, 5019 Monastir, Tunisia
[b] Department of Nanotechnology Engineering and Nanophotonics Research and Application Center, Sivas Cumhuriyet University, 58140, Sivas, Turkey
[c] Institut Supérieur des Sciences Appliqués et Technologie de Sousse, Université de Sousse, Tunisia
[d] Université de Toulouse, INSA-CNRS-UPS, LPCNO, Toulouse, France

ARTICLE INFO

Keywords:
Carrier localization
S-shape
Localized state ensemble (LSE)
InGaAs/InP
Photoluminescence
MOVPE

ABSTRACT

The free buffer InGaAs/InP structure has been elaborated by Metal Organic Vapor Phase Epitaxy (MOVPE). High indium content is chosen to reduce the bandgap energy of the ternary material with direct bandgap to be promoted for Infrared optoelectronic devices. In this work, the temperature dependent photoluminescence (TDPL) analysis of In-rich $In_xGa_{1-x}As$ (x = 0.65: S_1, x = 0.661: S_2, and x = 0.667 S_3) samples is of the central focus. The S-shaped behavior recorded at low temperature range in the III-V ternary is quantitatively studied herein by Localized State Ensemble (LSE) model. A comparison between the semi-empirical evolution of luminescence versus temperature and our numerical simulation proves the adequacy of computational details, used in LSE model, in well reproducing the S-shape feature. The numerical simulation well matched with PL spectra proving that the localization phenomenon is stronger when increasing the Indium mole fraction. The clustering effect in In-rich structure seems to be beneficial for enhancing the carrier localization within $In_xGa_{1-x}As$ by localizing carriers from away extended defects that behave probably as non-radiative centers. This is indicative of the utmost importance of localization phenomenon in trapping carriers within localized states instead of dislocations and defects, owing to clustering of indium atoms.

1. Introduction

Over the past decades, III-V compounds represent the most universally platform used in photonics. Their bandgap tunability reached via alloy engineering and their direct emission are considered the main operating characteristics that govern the optical devices' manufacturing. As an active layer, $In_xGa_{1-x}As$ ternary (noted InGaAs hereafter) is commonly chosen not only for most light emitting systems but also for photodetection application. Numerous investigations of such alloy have been devoted to ameliorating the growth conditions and to reach short-wave infrared (SWIR) frequencies by increasing Indium content in gallium arsenide [1,2]. Since the growth of InGaAs/GaAs highly introduces defects' density and misfit dislocations within the crystalline structure which will be degraded for higher Indium content [3], it has been demonstrated that engineering InGaAs lattice matched to InP can be ensured for Indium content x = 0.533 [4], aiming to reach the SWIR band. This finding is a landmark in the design of lattice-matching structures devoted to manufacturing optoelectronic devices operating in telecommunication and near infrared windows. However, carrier localization in such In-doped structures is extensively reported because of the highly In-induced compositional inhomogeneity in the host material (GaAs) and the high density of In-related impurities [5]. In fact, this aspect has been extended to several III-V alloys such as GaBiAs, GaSbBi, BGaAs, BInGaAs, GaInNAs, and InGaN due to the potential fluctuations induced near the band edge (conduction band-valence band) by the incorporation of Bismuth, Bore, Indium, and Nitrogen atoms [6–15]. This phenomenon is especially concretized by an anomalous temperature dependent photoluminescence. Eliseev et al. [15] developed a band-tail model to interpret the S-shape optically observed in InGaN material at low temperatures. Though the empirical formula well simulates the energy behavior at high temperatures, it still unable to describe this anomaly in the low temperature range. Then, Li

* Corresponding author.
E-mail address: benarbiamarwa94@gmail.com (M. Ben Arbia).

https://doi.org/10.1016/j.mssp.2021.106411
Received 29 May 2021; Received in revised form 29 November 2021; Accepted 14 December 2021
Available online 5 January 2022
1369-8001/© 2021 Published by Elsevier Ltd.

et al. proposed a Localized-State Ensemble (LSE) model well reproducing the InGaN's red-blue-red behavior for overall temperature range that was reduced to Eliseev et al.'s model at high temperatures [16]. This latter provides a quantitative analysis of steady-state photoluminescence which remains in use of several research works for studying the localization effect. The red-blue-red feature could be favorable for luminescent systems due to the localized centers that stimulate the radiative recombination process [17]. Exciton localization has been investigated in several scientific reports [18–21]. According to references [20,21], the random variation in the chemical composition of InGaAs alloy and/or inhomogeneity and roughness of barrier-well interfaces of InGaAs quantum wells seem like a trigger of the potential fluctuation. At low temperature, photo-created carriers are trapped at the potential minima. Poças et al. [20,21] have studied the localization phenomenon by performing a systematic assessment of the photoluminescence dependence on excitation intensity power and temperature for InGaAs/InAlAs grown on InP substrate. A blueshift of the emission energy is mentioned at low temperature (up to 30 K) as well as when increasing the excitation intensity, attributed to the potential fluctuation: after creation of excitons, carriers will be relaxed over the potential minima. This trend is explained by the contribution of non-localized excitons: when increasing temperature till $\leq$ 30 K, the thermal energy given to excitons localized in the potential minima is sufficient to activate the delocalized ones. However, when increasing temperature above 30 K the energy follows the bandgap behavior of InGaAs QW (redshift) because of the LO phonon scattering [22] where the main contribution is attributed to the non-localized excitons density [21].

Obviously, carrier localization is a key importance for alloys' optoelectronic properties. As a result of increasing Indium content, the clusters of In-atoms, the means by which the band tail-localized states are generated, contribute to the radiative recombination by both of transfer and redistribution mechanisms. In this context, the growth of InGaAs/InP without buffer layers was performed to obtain higher photoemission. We have carried out an optical investigation of In-rich InGaAs structures by stationary photoluminescence technique [23] showing an unusual luminescence behavior over the low temperature range. This behavior is detrimental for the SWIR application as it increases the dark current density [24]. In pursuit of this work, we make tremendous efforts through this paper to get in depth insight into the optical mechanism in such material by numerically developing the LSE model.

2. Methods

2.1. Experimental details

The 190 nm-InGaAs/InP heterostructure grown with Metal Organic Vapor Phase Epitaxial (MOVPE) was investigated for different Indium contents ($x = 0.65$ (S_1), 0.661 (S_2) and 0.667 (S_3)). Their optical investigation in the range 10 K–300 K performed by photoluminescence spectroscopy using excitation wavelength of 514.5 nm [23] will be used in this paper for the quantitative analysis of anomalous S-shape feature. All the growth and photoluminescence details were reported in reference [23].

2.2. Numerical approach: Localized State Ensemble (LSE)

Temperature dependence of intrinsic properties has already gained much interest in studying the physical phenomena within semiconducting materials. Several empirical models were devoted to study the energetic behavior versus temperature as mentioned as Varshni, Vina and Pässler models [25]. In response to the abnormal luminescence in such alloys, several attempts were made to simulate this kind of emission energy evolution. Eliseev et al. [15] have used equation (1) to interpret this phenomenon by expressing the temperature dependent energy $E(T)$:

$$E(T) = E_0 - \frac{\sigma^2}{K_B T} \tag{1}$$

Where E_0 is expected to be the energy peak position at T = 0 K, σ is the standard deviation of the localized states' distribution and K_B is the Boltzmann parameter.

However, equation (1) is useful only at temperature higher than 77 K [15]. Another model is developed to reproduce the S-shape feature known as "Localized State Ensemble Model (LSE)". The distribution function $f(E,T)$ and the Gaussian-type density of states ω^{DOS} , given in equations (2) and (3) are used in this model to describe quantitatively the variation of the emission peaks versus temperature [16].

$$f(E,T) = \frac{1}{e^{\frac{E-E_0}{K_B T}} + \frac{\tau_{tr}}{\tau_r}} \tag{2}$$

$$\omega^{DOS}(E) = \omega_0 e^{\frac{-(E-E_0)^2}{2\sigma^2}} \tag{3}$$

Where τ_r and τ_{tr} symbolize respectively the radiative recombination lifetime and the escape lifetime of localized carriers. The ratio $\frac{\tau_r}{\tau_{tr}}$ governs the carrier localization and ω_0 represents the amplitude of DOS distribution.

The steady-state luminescence spectra evolution of the localized carriers depending on the sample temperature is given by equation (4.1):

$$\chi(E,T) = \omega^{DOS}(E) f(E,T) \tag{4.1}$$

The derivative of this function, with respect to the energy, $\frac{\partial \chi}{\partial E} = 0$ only for

$$E = E_0 - \mu(T).K_B T \tag{4.2}$$

The coefficient μ, as a function of temperature T, represents the thermal redistribution of carriers over states associated to localized defects, which is estimated by LSE model as $0 < \mu < \left(\frac{\sigma}{K_B T}\right)^2$ by solving equation (5):

$$\mu e^{\mu} = \left[\left(\frac{\sigma}{K_B T}\right)^2 - \mu\right]\left(\frac{\tau_r}{\tau_{tr}}\right) e^{\frac{E_0 - E_a}{K_B T}} \tag{5}$$

In LSE frame, E_0 and E_a are estimated to be the central energy of the localization states' distribution and the energetic position below which carriers occupy the localization states at T = 0 K, respectively.

The equation (4.2) can be expressed for an ideal semiconductor by the semi empirical Pässler model as the following [11]:

$$E = E_0 - \frac{\alpha \Theta_D}{2}\left[\sqrt[\upsilon]{1 + \left(\frac{2T}{\Theta_P}\right)^{\upsilon}} - 1\right] - \mu(T).K_B T \tag{6}$$

The parameters derived from the second term that describes the bandgap energy shrinkage are represented herein:

α designates the derivative of energy with respect to the temperature for limit value of high temperature such that $\alpha = -\frac{dE}{dT_{T\to\infty}}$ [11].

Θ_P is estimated to be the average phonon temperature.

$\upsilon = \sqrt{1 + \left(\frac{\Delta\varepsilon}{\varepsilon}\right)^{-2}}$ represents the fractional exponent related to the phonon dispersion where $\frac{\Delta\varepsilon}{\varepsilon}$ is the phonon dispersion degree.

The exponent υ is meaningful for the phonon spectral distribution according to Pässler model [26], where we distinguish three regimes:

$\upsilon < 2$: regime of large dispersion.

$2 < \upsilon < 3.3$: regime of intermediate dispersion.

$\upsilon > 3.3$: regime of small dispersion.

At high temperatures, the energy evolution follows the band-tail

model or Eliseev's model where the parameter $\mu(T) = \left(\frac{\sigma}{K_B T}\right)^2$.

The integrated intensity of luminescence in LSE model is connected to the density of localized carriers as [27]:

$$I(T)\ \alpha \int_{-\infty}^{+\infty} f(E,T).\omega^{DOS}(E)dE \quad (7)$$

We therefore have

$$I(T)\ \alpha\ 1 \Bigg/ \left\{1+(1-\gamma_c).\exp\left(\frac{E_a - E_0 + K_B T \ln\left(\frac{\tau_r}{\tau_{tr}}\right)}{\sqrt{(K_B T)^2 + 2\left(\frac{\sigma}{2.41}\right)^2}}\right)\right\} \quad (8)$$

by using the approximation indicated below:

$$\int_{-\infty}^{+\infty} \frac{e^{-x^2}}{1+e^{a_0(x+b_0)}} dx \approx \frac{\sqrt{\pi}}{1+e^{2.41\ b_0 \sin(\arctan(a_0/2.41))}} \quad (9)$$

It is well to know that the coefficient γ_c defines the recapture of carriers by localized centers.

3. Results and discussion

The photoluminescence spectroscopy of samples S_1, S_2 and S_3 was performed at low temperature proving the operation of the investigated structure InGaAs in Short Wavelength Infra-Red (SWIR) region, as exhibits Fig. 1 [23].

From this figure, firstly, we can see that the emission energy is redshifted with increasing the Indium concentration owing to the difference in atomic radii and electronegativities for Gallium and Indium atoms.

Since 1983 [28], the indium has been introduced in the bulk GaAs crystal to reduce the dislocations density. Laurenti et al. [29] have studied a set of GaAs samples by photoluminescence spectroscopy showing shifts in the energy position to lower values when increasing the indium concentrations. They have justified this redshift by "the formation of a very dilute InGaAs ternary compound" [30]. In Fig. 2, we describe this phenomenon schematically. The incorporation of indium atoms will substitute the gallium ones within the host matrix GaAs. The different atomic size and electronegativity of both the atoms (Ga, In) will

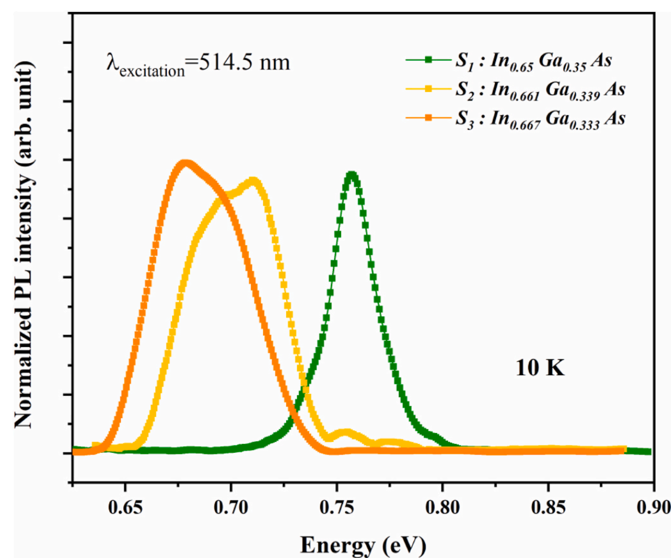

Fig. 1. Spectral evolution of photoluminescence emission of the samples S_1, S_2, and S_3 with Indium content of 0.65, 0.661, and 0.667 at low temperature.

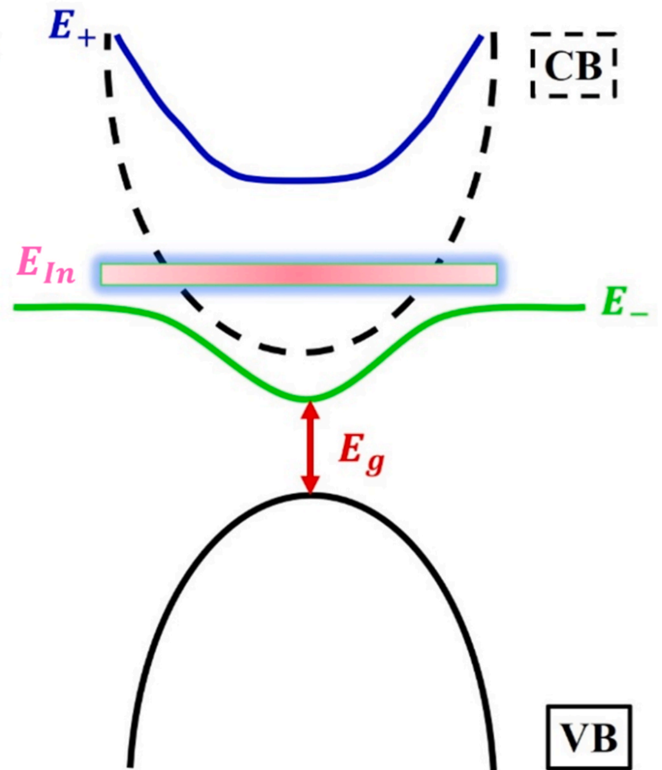

Fig. 2. Bandgap energy reduction of GaAs after Indium incorporation: the dilute-alloyed systems [31].

induce an isoelectronic level that will be in interaction with the conduction band (CB) leading to a splitting of the CB into two subbands E_+ and E_- that reduce consequently the bandgap energy (redshift) [31]. The same feature (redshift) is mentioned for Indium rich InGaAs/InP. However, the Indium in this case has a full contribution in the composition of pseudo-binary compound and cannot act as substitutional impurity. The variation of bandgap energy in the In-alloyed system is governed by the Vegard law where the band gap energy E_g of a random alloy $AB_{1-x}C_x$ is described by the function as follows:

$$E_g(x) = (1-x).\ E_g^{AB} + x.\ E_g^{AC} - b.\ x.\ (1-x)$$

E_g^{AB} and E_g^{AC} are the bandgap energies of the binary constituents, b is the bowing factor set at 0.494 eV for InGaAs, and x is the indium composition [32].

Kuphal et al. have demonstrated that the incorporation of indium atoms into the GaAs matrix can affect the lattice parameter and reduce the bandgap energy of GaAs, as proved by XRD and photoluminescence measurements [32].

To more explain the redshift of bandgap energy after the Indium incorporation into the Gallium arsenide, Laurenti et al. [29] have investigated the near-band-edge optical transitions. They have reported that Indium not only improves the luminescence intensity but also shifts the emission peaks towards low energies (16.8 meV per 1% of indium content). Based on the general crystal-field theory, the observed redshift finds its origin in the change of magnitude of crystal-field splitting which is related to the lattice parameters of GaAs and InGaAs described by the formula below:

$$\Delta E = E_{GaAs}.\left[\left(\frac{a_{GaAs}}{a_{InGaAs}}\right)^5 - 1\right]$$

It is well to be noted that the Indium fills the clusters surrounding the defects and residual impurities within the host material GaAs leading to relaxing the lattice distortions. This will lower the total energy of the overall system, hence reducing the dislocations density. However, when

the incorporation of Indium exceeds 53%, a considerable number of structural defects can be formed as reported in our previous work [23]. Secondly, comparing S_2 and S_3 to S_1, the spectral evolution of PL emission reveals a widen PL band owing to the further increase in In incorporation that may be related to the inhomogeneous distribution and the interface roughness in InGaAs/InP [25]. Foreseeing to get in-depth assessment of optical behavior in such structure, a temperature-dependent photoluminescence (TDPL) investigation of InGaAs/InP was performed by PL spectroscopy as mentioned in Ref. [23], showing that the emission of the active layer spans the range 1500–2000 nm for different mole fraction $x = 0.65$ (S_1), 0.661 (S_2) and 0.667 (S_3). An S-shape behavior was recorded at low temperatures and reproduced numerically in this paper using the Localized State Ensemble model. Fig. 3, Fig. 4, and Fig. 5 depict the simulation of PL emission peak positions versus temperature using both of semi empirical Pässler model and LSE model as addressed in the preceding subsection.

The thermal evolution of PL intensities is also exposed in Fig. 6 for the three samples and numerically fitted by LSE model. All fitting parameters are summarized in Table 1.

For comparison, the Pässler- and LSE-fitting parameters are shown in Table 2, where the simulation notably exhibits a complete congruence at higher temperature range.

The phonon dispersion degree so as $2 < \upsilon < 3.3$ in the Pässler model is assigned with the intermediate dispersion regime. Yet, in the LSE representation $\upsilon > 3.3$ is pertained to the small dispersion regime where the LO-phonon distribution dominates the LA-phonon one. As shown, the high values of $\alpha^{\text{Pässler}}$ and $\Theta_P^{\text{Pässler}}$ are considered as a proof of localization phenomenon, reported by Dixit et al. in Ref. [25]. Here, the developed LSE model succeed to replicate the S-shaped form by adjusting all the physical parameters, favorable to assess the localization phenomenon. In other terms, the comparison between Pässler and LSE models is effectuated to justify the utility of using the quantitative LSE model through which an agreement considerably shown between the experimental results and the numerical ones, demonstrating the validation of our model and the accuracy of parameters used herein. It is notable that the LSE simulation reproduces well the S-shape in the low temperature regime, where the localization degree is higher as the Indium content is increased. Based on our fitting results, presented in Figs. 3, Fig. 4, and Fig. 5 we can conclude that the LSE model is well adapted to our samples. This is proving that the localization is highly sensitive to the Indium concentration in such alloy. A further increase in Indium content reduces the density of localized states by intervening

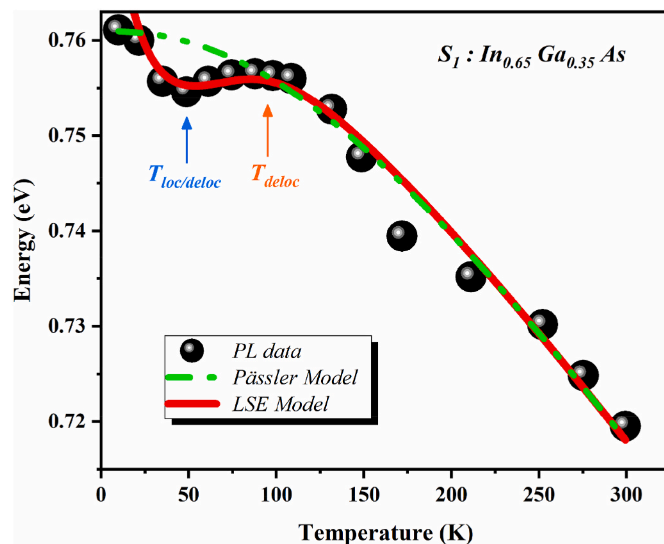

Fig. 3. Temperature dependence of steady-state photoluminescence energy for S_1: Comparison between semi-empirical Pässler model and LSE model.

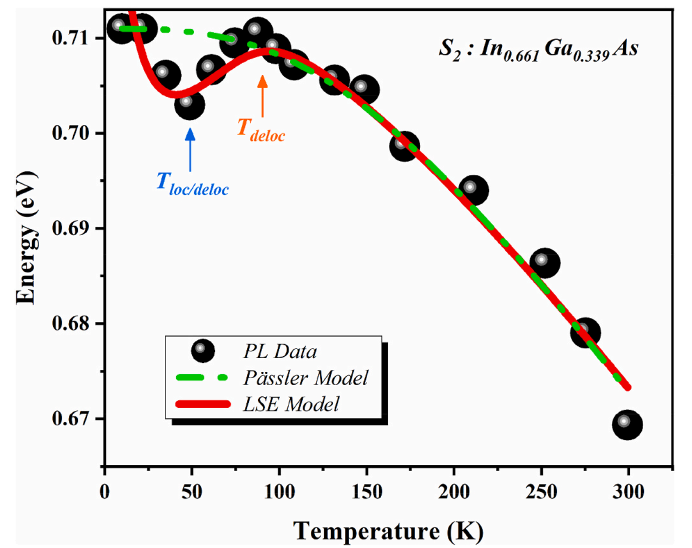

Fig. 4. Temperature dependence of steady-state photoluminescence energy for S_2: Comparison between semi-empirical Pässler model and LSE model.

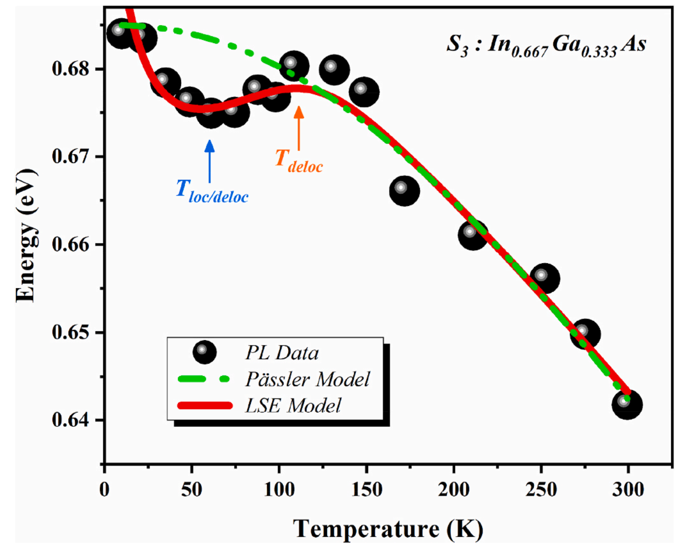

Fig. 5. Temperature dependence of steady-state photoluminescence energy for S_3: Comparison between semi-empirical Pässler model and LSE model.

more non-radiative defects. In general, compositional fluctuation, thickness fluctuation in quantum wells and built-in electric field in polar structures are the main causes behind localization phenomenon [33,34]. Herein, the observed localization in TDPL spectra for the three samples is mostly due to the fluctuation in In composition since the uncapped InGaAs grown on InP are only distinguishable with respect to the Indium content where its variation from 0.65 to 0.667 changes reasonably the S-shaped form. Resembling the Fermi energy E_f in quantum mechanics, E_a has a decisive influence in studying the carrier localization for luminescent system [35]. It represents the level below which all carriers occupied the localized states at 0 K. The energetic difference $E_a - E_0$ estimated by LSE modeling is comparable with the thermal activation energy calculated by using Arrhenius plot in Ref. [23] ($E_a - E_0$ Vs. $E_a^{Arrhenius}$: S_1 : 16.70 meV Vs. 15.23 meV; S_2 : 24.26 meV Vs. 22.77 meV; and S_3 : 29.30 meV Vs. 27.64 meV). The comparability between these estimated energetic terms can justify the hypothesis that:

(I) Thermal activation energy (in Arrhenius plot) seems to be the energy required to activate the localized states ($E_a - E_0$).

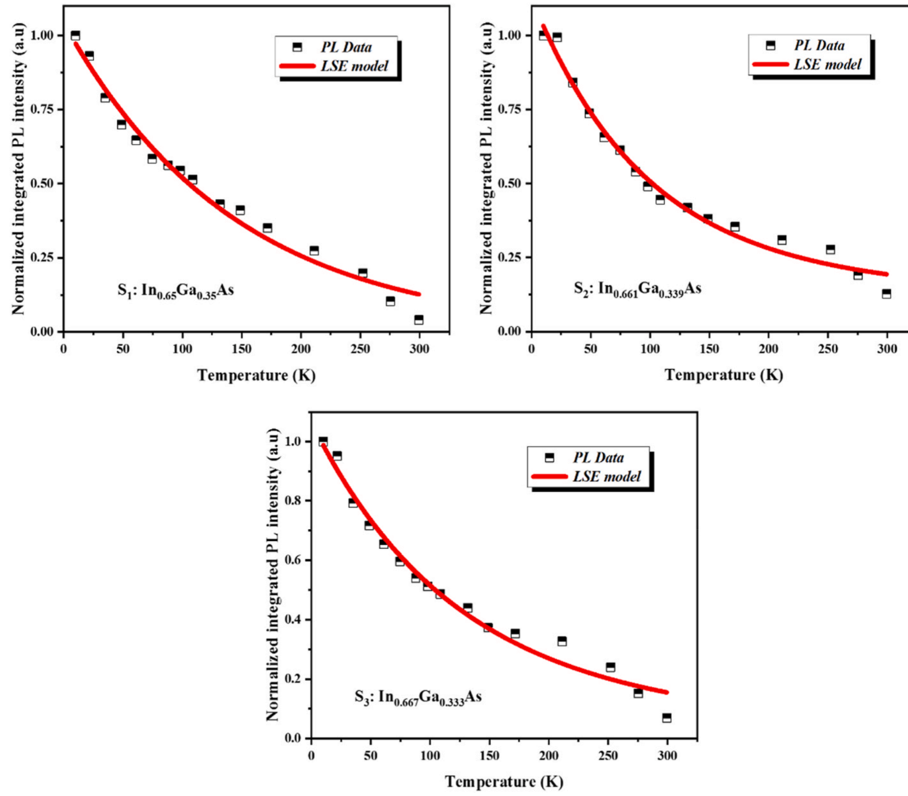

Fig. 6. Temperature dependence of photoluminescence intensity for S_1, S_2, and S_3 simulated according to LSE configuration.

Table 1
Summary of main characteristics governing the localization phenomenon in InGaAs/InP fitted by Localized States Ensemble model for Indium content $x = 0.65$, 0.661 and 0.667 corresponding to S_1, S_2 and S_3, respectively.

Sample	S_1	S_2	S_3
E_0 $(.10^{-3}eV)$	790	748	708
$E_a - E_0$ $(.10^{-3}eV)$	16.70	24.26	29.30
σ (meV)	4.8	11	16.5
τ_r/τ_{tr}	3154/0.4 = 7885	3825/0.3 = 12750	5242/0.6 ≅ 8737
γ_c	0.87	0.96	0.80
α $(.10^{-4}\ eV/K)$	2.70	2.73	2.60
Θ_P (K)	200	185	243
υ	6.2	9	9

Table 2
Comparison between fitting parameters of both semi-empirical Pässler model and Localized States Ensemble model for Indium content $x = 0.65$, 0.661 and 0.667 corresponding to S_1, S_2 and S_3, respectively.

Sample	S_1	S_2	S_3
$E_0^{Pässler}$ $(.10^{-3}eV)$	761	711	682
E_0^{LSE} $(.10^{-3}eV)$	790	748	708
$\alpha^{Pässler}(.10^{-4}\ eV/K)$	4	4.1	7.8
$\alpha^{LSE}(.10^{-4}\ eV/K)$	2.70	2.73	2.60
${\Theta_P}^{Pässler}(K)$	246	215	341
${\Theta_P}^{LSE}(K)$	200	185	243
$\upsilon^{Pässler}$	2.26	3	3
υ^{LSE}	6.2	9	9

(II) Radiative recombination defects are energetically laying well-nigh the level of the energy activation of localized states. (Defects and localized states have closely energetic level positions).

More precisely, the fact that $E_a - E_0$ is slightly more than the Arrhenius thermal energy $E_a^{Arrhenius}$ is justified by Li et al. [16]: Carriers need more thermal energy to be localized in the low temperature range compared to the high temperature range where defects and impurities

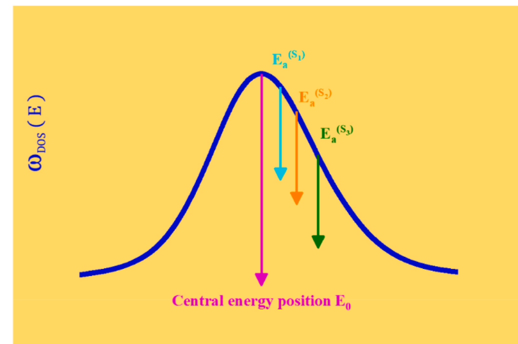

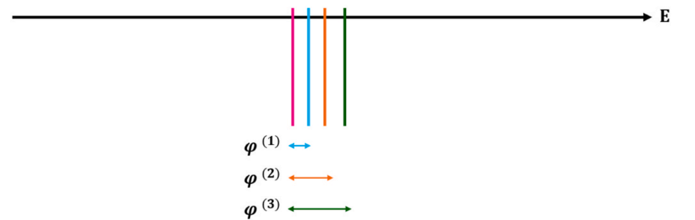

Fig. 7. Schematic representation of the distribution DOS of localized states at low temperature describing the energetic magnitude E_a-E_0 by indication of $\varphi^{(1)}$ (S_1); $\varphi^{(2)}$ (S_2); and $\varphi^{(3)}$ (S_3) regarding the central energy peak E_0.

thermally activated are often quench the PL intensity due to their non-radiative recombination nature. Since $E_a - E_0$ takes a positive value, E_a energetically lays above E_0 level. In Fig. 7, the distribution over the localized states of DOS function, ω^{DOS} is schematized by highlighting the energetic levels E_0 and E_a. Added to this, the

enlargement of $\tau_r/_{\tau_{tr}}$ by several orders of magnitude, when increasing Indium concentration, is a signature of the probability that carriers have to escape out of localized states [35]. This trend, probably associated with S_3, can be explained by the dislocation effect resulted in trapping carriers from localized states as it includes the highest value of both Indium content and dislocation density, thus the largest escape rate.

The increase in $E_a - E_0$ magnitude with the Indium content can justify the strong localization for higher concentrations of Indium at low temperature [26]. Added to $E_a - E_0$ energy, the temperature parameter T_{deloc} is of importance in studying the localization phenomenon. From Figs. 3, Fig. 4, Fig. 5 and Table 3, we extract the smaller value of T_{deloc} (90 K) which implies that samples S_1 and S_2 take precedence in term of delocalizing carriers over the sample S_3: the trapped carriers begin to leave the localization states in S_1 and S_2 at 90 K, before S_3 (110 K), highlighting the dominance of localization process over the delocalization one. This finding is emphasized by the large localization degree ($\sigma = 16.5\, meV$) associated with the third sample S_3. Compared to Fraj et al.'s research works [36], the estimated localization degree ($\sigma = 4.8\, meV;\ 11\, meV;\ 16.5\, meV$) is higher than InGaAs/GaAs with 23% of In content ($\sigma = 2\, meV\, ;3\, meV$). This is expected due to the important Indium concentrations ($\geq 65\%$) within the InGaAs/InP structures.

To make these anomalous TDPL shifts more understandable, we elucidate in Fig. 8 how the localized states play on photoluminescence mechanism through three processes: (1): The first redshift occurs when carriers are trapped in deepest level of localization states. Upon increasing temperature, the localized carriers were redistributed within potential minima leading to (2) a blueshift of emission energy where carriers reach shallower localized states. Further increase in temperature allows (3) a second redshift where the weakly localized carriers escape from the potential minima through the delocalization process.

As the thermal redistribution of carriers is the responsible of the energy blueshift resulted in S-shaped luminescence, distinguishable at low temperatures, the dimensionless term $\mu(T)$, multiplied by the thermal energy K_BT, is quantitatively described in Fig. 9.

This parameter reflects the competition between localization and delocalization effects by highlighting two characteristic temperatures $T_{loc/deloc}$: the temperature at which the maximal redshift is recorded, and T_{deloc}: the temperature at which the blueshift attain its maximum. From the graph and the thermal dependence of photoluminescence shown in Figs. 3, Fig. 4, and Fig. 5, the critical parameters for localization procedure are listed in Table 3 for the three samples. The curves describing the thermal redistribution in Fig. 9 show that carriers are incompletely delocalized in all the samples (as indicates the vertical dashed line). Hidouri et al. referred this incomplete process to the low thermal energy that carriers can gain to be totally delocalized from potential minima [36]. To investigate the localization influence on InGaAs emissivity, the estimation of internal quantum efficiency (IQE) needs to presume that non-radiative centers do not contribute to the recombination process (supposed to behave as frozen centers at 10 K) [36]. In this context, IQE is given in Table 3 for the three samples by calculating the PL intensity

Table 3
Critical parameters related to carrier localization in In-rich InGaAs alloy.

Sample	S_1	S_2	S_3
$T_{loc/deloc}$ (K)	50	50	60
T_{deloc} (K)	90	90	110
σ (meV)	4.8	11	16.5
γ_c	0.87	0.96	0.80
IQE (%)	4.02	12.39	6.10

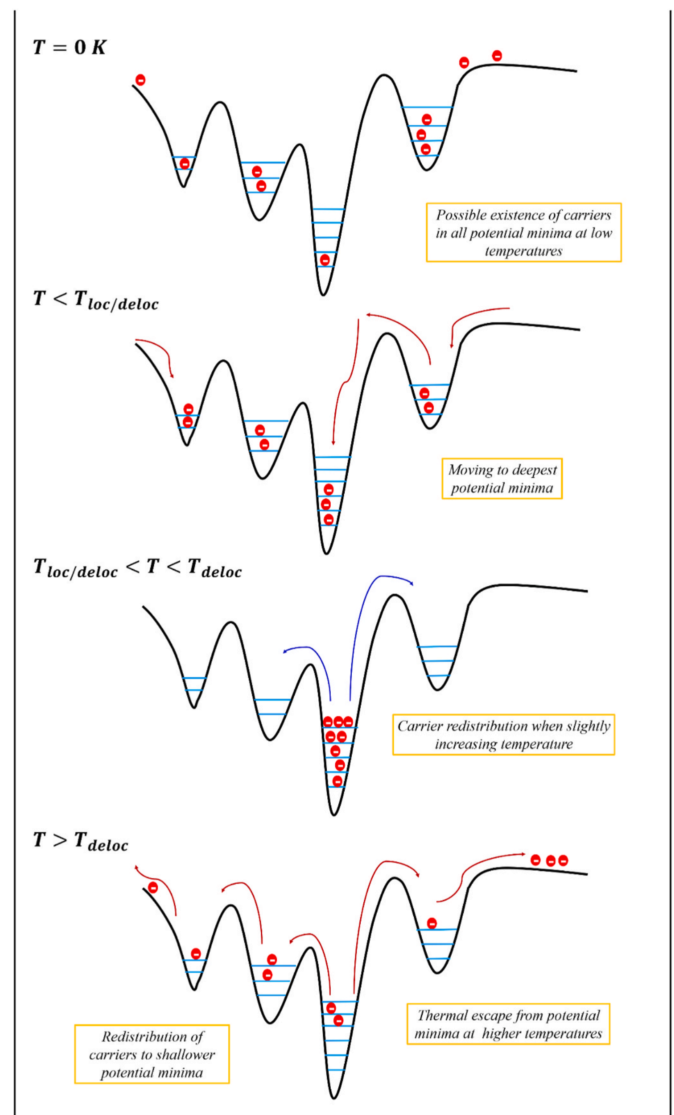

Fig. 8. Localization mechanism in In-rich ternary: Schematic diagrams to describe the carrier distribution when increasing temperature.

ratio at the lowest and the highest temperatures during PL experiments (10 K and 300 K in this work), described by this equation [37]:

$$IQE = \frac{I_{PL}^{300\ K}}{I_{PL}^{10\ K}} \quad (10)$$

Noticeably, we record the highest value of IQE for S_2 compared to both S_1 and S_3. Localization enhances the light efficiency when comparing S_1 to S_2. However, the drop in IQE is recorded when increasing the Indium content by 0.6% despite of the strong localization degree estimated for S_3. This can be attributed to the high densities of defects and dislocations introduced by the incorporation of Indium content $x > 0.53$ which in turn enhances the clustering of In atoms [37–40]. Indeed, Dong et al. [38] attributed the rise of internal quantum efficiency to the enhanced periodicity in III-V alloy when increasing the Indium content resulted in the increase of total accumulated strain. To our knowledge, the growth of heterostructure InGaAs on InP with the In concentration exceeding 0.53 allows the lattice mismatch resulted in inducing strain, defects and dislocations into the samples [41]. A structural analysis using XRD and Raman scattering techniques proved high dislocation densities: $2.17\,10^9\ cm^{-2}$ (S_1), $2.64\,10^9\ cm^{-2}(S_2)$, and $3.14\,10^9\ cm^{-2}(S_3)$ and large residual strain: $2.88\,GPa\,(S_1)$, $3.80\,GPa\,(S_2)$, and $4.17\,GPa\,(S_3)$ when increasing the Indium mole

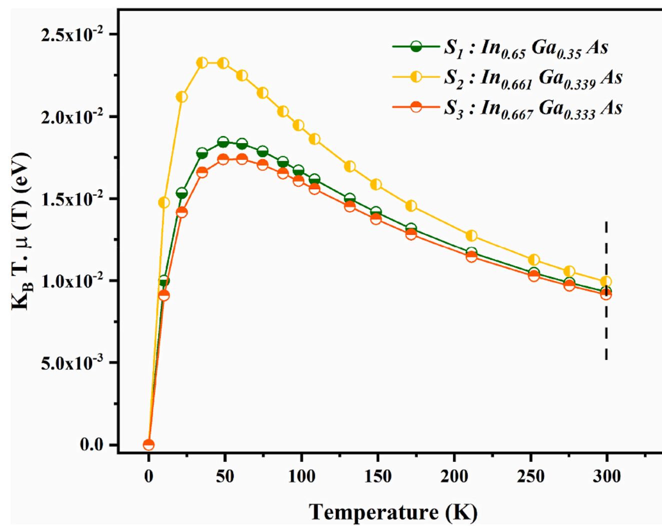

Fig. 9. Amplitude of the term μ(T)*K_BT describing the thermal redistribution of carriers in InGaAs for different Indium content x = 0.65, x = 0.661 and x = 0.667.

fraction in this ternary [33]. These findings supposed to degrade the optical properties by quenching the light emission in semiconductors whose dislocation density exceeded $10^3\ cm^{-2}$. However, we observed a contrarian phenomenon in In-rich InGaAs material that still emit even tough at high density of dislocations ($10^9\ cm^{-2}$). Similarly, Humphreys [42] recorded the same trend in In-rich InGaN with $10^9\ cm^{-2}$ of dislocations' densities. This result finds a solid interpretation in the "carrier escape from dislocations to localized states" process [42,43], activated via In-rich clusters in InGaAs structure.

The IQE is enhanced by 8.37% when increasing the Indium content from 0.65 to 0.661. However, the further increase in Indium content to 0.667 degrades the efficiency from 12.39% to 6.10% but still higher than that associated with S_1. The drop in luminescence efficiency for S_3 can be related to the higher dislocation density ($3.14\ 10^9\ cm^{-2}$) compared to S_2 ($2.64\ 10^9\ cm^{-2}$). In addition, despite the large localization degree in S_3, the IQE exhibits a diminution compared to S_2 that may be related to the recapture coefficient γ_c whose value is lower when increasing Indium content by 0.6%: Carriers have probability to be re-captured by localized states in S_2 more efficiently than S_3, hence empowering the light efficiency. To sum up, the interplay between localized states and dislocation density strongly governs the photoluminescence efficiency where Indium composition enhances the IQE ratio. Nevertheless, at a specific concentration, dislocations can affect the localization phenomenon resulting in reducing the localization effects and quenching the light emission as shown in Fig. 6. In point of physical view, the anomalous thermal evolution of emission energy manifested in S-shape is a fingerprint of carrier localization phenomenon within III-V alloys [36, 44,45]. In fact, the incorporation of Indium into GaAs favors the segregation phenomenon that induces In-rich zones resulted in In-clusters due to its positionally random distribution and to the energetic disorder related to the alloying systems [36,46,47]. By these properties we justify the localization phenomenon coming in form of S-shaped behavior in our samples. The inhomogeneous carrier distribution within In-rich structure can be managed by multiple kinds of localized states: isolated In-related states, InAs Quantum dots (QDs), In-clusters QDs-like [22], impurities during the growth process such as nitrogen and hydrogen that it has already used as carrier gases in MOVPE system. Eliseev et al. favor the theory of randomly self-formed QDs in In_xGa_{1-x} N (x = 0.3 and x = 0.45) due to the Indium compositional fluctuation that gives arise to local potential for carriers to be localized there [15].

4. Conclusion

In this paper, we performed an optical study of In-rich InGaAs that revealed an anomalous evolution when increasing temperature, endowing the S-shaped form. This is a fingerprint of localized carriers owing to the composition fluctuation and the alloy disorder. A quantitative investigation of such behavior was devoted to reproducing the S-shape by LSE model allowing the extraction of the accurate physical parameters numerically. We demonstrated herein that the localization degree is more important as well as the Indium content is increased. Accordingly, the localization phenomenon seemed to be behind the enhancement of the luminous efficiency by almost 8.37% when increasing the Indium content by 1.1% even for higher dislocation density. However, we remarked that a further increase in the Indium concentration enhanced the localization degree but also generated a high density of dislocations in sample S_3 (66.7%) that degrades the luminescence efficiency. Added to the study of ternary's PL behavior for different Indium contents, this work provided the optimal concentration of Indium in simple structure of InGaAs/InP without buffer layer that ensured higher luminescence efficiency (66.1% Vs. 65% and 66.7%).

Declaration of competing interest

The authors declare that they have no known competing financial interests or personal relationships that could have appeared to influence the work reported in this paper.

References

[1] Y. Arslan, F. Oguz, C. Besikci, Extended wavelength SWIR InGaAs focal plane array: characteristics and limitations, Infrared Phys. Technol. 70 (2015) 134–137.
[2] F. Rutz, P. Kleinow, R. Aidam, W. Bronner, L. Kirste, M. Walther, October) InGaAs infrared detector development for SWIR imaging applications, in: Electro-Optical and Infrared Systems: Technology and Applications X, vol. **8896**, International Society for Optics and Photonics, 2013, p. 88960C.
[3] P.R. Griffin, J. Barnes, K.W.J. Barnham, G. Haarpaintner, M. Mazzer, C. Zanotti-Fregonara, E. Grünbaum, C. Olson, C. Rohr, J.P.R. David, J.S. Roberts, R. Grey, M. A. Pate, Effect of strain relaxation on forward bias dark currents in GaAs/InGaAs multiquantum well p–i–n diodes, J. Appl. Phys. 80 (10) (1996) 5815–5820.
[4] M.L. Huang, S.W. Chang, M.K. Chen, C.H. Fan, H.T. Lin, C.H. Lin, R.L. Chu, K. Y. Lee, M.A. Khaderbad, Z.C. Chen, C.H. Lin, C.H. Chen, L.T. Lin, H.J. Lin, H. C. Chang, C.L. Yang, Y.K. Leung, Y.-C. Yeo, S.M. Jang, H.Y. Hwang, C.H. Diaz, June) in 0.53 Ga 0.47 as MOSFETs with high channel mobility and gate stack quality fabricated on 300 mm Si substrate, in: 2015 Symposium on VLSI Technology (VLSI Technology), 2015, pp. T204–T205 (IEEE).
[5] Q.D. Zhuang, J.M. Li, Y.P. Zeng, S.F. Yoon, H.Q. Zheng, M.Y. Kong, L.Y. Lin, Effect of rapid thermal annealing on InGaAs/GaAs quantum wells, J. Cryst. Growth 212 (1–2) (2000) 352–355.
[6] R. Kudrawiec, M. Syperek, P. Poloczek, J. Misiewicz, R.H. Mari, M. Shafi, M. Henini, Y. Galvão Gobato, S.V. Novikov, J. Ibáñez, M. Schmidbauer, S.I. Molina, Carrier localization in GaBiAs probed by photomodulated transmittance and photoluminescence, J. Appl. Phys. 106 (2) (2009), 023518.
[7] T. Hidouri, I. Mal, D.P. Samajdar, F. Saidi, T.D. Das, Impact of localization phenomenon and temperature on the photoluminescence spectra of GaSbBi alloys and GaSbBi/GaAs quantum dots, Superlattice. Microst. 129 (2019) 252–258.
[8] T.D. Das, D.P. Samajdar, M.K. Bhowal, S.C. Das, S. Dhar, Photoluminescence studies of GaSbBi quantum dots grown on GaAs by liquid phase epitaxy, Curr. Appl. Phys. 16 (12) (2016) 1615–1621.
[9] M. Ezzedini, T. Hidouri, M.H.H. Alouane, A. Sayari, E. Shalaan, N. Chauvin, L. Sfaxi, F. Saidi, A. Al-Ghamdi, C. Bru-Chevallier, H. Maaref, Detecting spatially localized exciton in self-organized InAs/InGaAs quantum dot superlattices: a way to improve the photovoltaic efficiency, Nanoscale Res. Lett. 12 (1) (2017) 1–10.
[10] T. Hidouri, F. Saidi, H. Maaref, P. Rodriguez, L. Auvray, Localized state exciton model investigation of B-content effect on optical properties of BGaAs/GaAs epilayers grown by MOCVD, Vacuum 132 (2016) 10–15.
[11] T. Hidouri, F. Saidi, H. Maaref, P. Rodriguez, L. Auvray, Impact of photoluminescence temperature and growth parameter on the exciton localized in BxGa1-xAs/GaAs epilayers grown by MOCVD, Opt. Mater. 60 (2016) 487–494.
[12] T. Hidouri, F. Saidi, H. Maaref, P. Rodriguez, L. Auvray, LSE investigation of the thermal effect on band gap energy and thermodynamic parameters of BInGaAs/GaAs single quantum well, Opt. Mater. 62 (2016) 267–272.
[13] L. Grenouillet, C. Bru-Chevallier, G. Guillot, P. Gilet, P. Duvaut, C. Vannuffel, A. Chenevas-Paule, Evidence of strong carrier localization below 100 K in a GaInNAs/GaAs single quantum well, Appl. Phys. Lett. 76 (16) (2000) 2241–2243.
[14] R. Belghouthi, J.P. Salvestrini, M.H. Gazzeh, C. Chevallier, Analytical modeling of polarization effects in InGaN double hetero-junction pin solar cells, Superlattice. Microst. 100 (2016) 168–178.

[15] P.G. Eliseev, P. Perlin, J. Lee, M. Osiński, "Blue" temperature-induced shift and band-tail emission in InGaN-based light sources, Appl. Phys. Lett. 71 (5) (1997) 569–571.
[16] Q. Li, S.J. Xu, W.C. Cheng, M.H. Xie, S.Y. Tong, C.M. Che, H. Yang, Thermal redistribution of localized excitons and its effect on the luminescence band in InGaN ternary alloys, Appl. Phys. Lett. 79 (12) (2001) 1810–1812.
[17] C.J. Collins, A.V. Sampath, G.A. Garrett, W.L. Sarney, H. Shen, M. Wraback, A. Yu Nikiforov, G.S. Cargill III, V. Dierolf, Enhanced room-temperature luminescence efficiency through carrier localization in Al x Ga 1− x N alloys, Appl. Phys. Lett. 86 (3) (2005), 031916.
[18] Q. Yang, J. Chen, A. Li, Photoluminescence study of InGaAs/InAlAs single and multiple quantum wells, J. Cryst. Growth 194 (1) (1998) 31–36.
[19] Y. Wang, X. Sheng, Q. Guo, X. Li, S. Wang, G. Fu, Y.I. Mazur, Y. Maidaniuk, M. E. Ware, G.J. Salamo, B. Liang, D.L. Huffaker, Photoluminescence study of the interface fluctuation effect for InGaAs/InAlAs/InP single quantum well with different thickness, Nanoscale Res. Lett. 12 (1) (2017) 1–9.
[20] L.C. Poças, J.L. Duarte, E.M. Lopes, I.F.L. Dias, E. Laureto, D.F. César, J. C. Harmand, The effect of potential fluctuations on the optical properties of in Ga As/ in Ga Al as single and coupled double quantum wells, J. Appl. Phys. 100 (5) (2006), 053519.
[21] L.C. Poças, E.M. Lopes, J.L. Duarte, I.F.L. Dias, S.A. Lourenço, E. Laureto, M. Valadares, P.S.S. Guimarães, L.A. Cury, J.C. Harmand, The effect of potential fluctuations on the optical properties of in Ga As/ in Al as superlattices, J. Appl. Phys. 97 (10) (2005) 103518.
[22] T. Hidouri, F. Saidi, B.M. Al-Shahri, Tuning spontaneous emission in BInGaAs/GaAs QWs by varying the growth temperature: above 1.2 μm emission and solar cells application, Opt. Quant. Electron. 53 (9) (2021) 1–13.
[23] B. Smiri, M. Ben Arbia, D. Ilkay, F. Saidi, Z. Othmen, B. Dkhil, A. Ismail, E. Sezai, F. Hassen, H. Maaref, Optical and structural properties of In-rich InxGa1− xAs epitaxial layers on (1 0 0) InP for SWIR detectors, Mater. Sci. Eng., B 262 (2020) 114769.
[24] X. Ji, B. Liu, Y. Xu, H. Tang, X. Li, H. Gong, B. Shen, X. Yang, P. Han, F. Yan, Deep-level traps induced dark currents in extended wavelength InxGa1− xAs/InP photodetector, J. Appl. Phys. 114 (22) (2013) 224502.
[25] V.K. Dixit, S. Porwal, S.D. Singh, T.K. Sharma, S. Ghosh, S.M. Oak, A versatile phenomenological model for the S-shaped temperature dependence of photoluminescence energy for an accurate determination of the exciton localization energy in bulk and quantum well structures, J. Phys. Appl. Phys. 47 (6) (2014), 065103.
[26] T. Hidouri, R. Hamila, F. Saidi, H. Maaref, P. Rodriguez, L. Auvray, Investigation of the localization phenomenon in quaternary BInGaAs/GaAs for optoelectronic applications, Superlattice. Microst. 103 (2017) 386–394.
[27] Q. Li, S.J. Xu, W.C. Cheng, M.H. Xie, S.Y. Tong, A model for steady-state luminescence of localized-state ensemble, EPL (Europhysics Letters) 71 (6) (2005) 994.
[28] G. Jacob, M. Duseaux, J.P. Farges, M.M.B. van den Boom, P.J. Roksnoer, J. Cryst. Growth 61, 417. Dislocation-free GaAs and InP Crystals by Isoelectronic Doping, 1983.
[29] J.P. Laurenti, P. Roentgen, K. Wolter, K. Seibert, H. Kurz, J. Camassel, Improvement of GaAs epitaxial layers by indium incorporation, J. Phys. Colloq. 49 (C4) (1988) C4–C693.
[30] J.P. Laurenti, P. Roentgen, K. Wolter, K. Seibert, H. Kurz, J. Camassel, Indium-doped GaAs: a very dilute alloy system, Phys. Rev. B 37 (8) (1988) 4155.
[31] M. Ben Arbia, H. Helal, F. Saidi, H. Maaref, Investigation of 1.9 μm GINA simulated as intrinsic layer in a GaAs homojunction: from 25% towards 32.4% conversion yield, J. Electron. Mater. 49 (11) (2020) 6308–6316.
[32] E. Kuphal, A. Pöcker, A. Eisenbach, Relation between photoluminescence wavelength and lattice mismatch in metalorganic vapor-phase epitaxy InGaAs/InP, J. Appl. Phys. 73 (9) (1993) 4599–4604.
[33] Q. Li, S.J. Xu, M.H. Xie, S.Y. Tong, Origin of the 'S-shaped' temperature dependence of luminescent peaks from semiconductors, J. Phys. Condens. Matter 17 (30) (2005) 4853.
[34] M.J.S.P. Brasil, A.A. Bernussi, M.A. Cotta, M.V. Marquezini, J.A. Brum, R. A. Hamm, S.N.G. Chu, L.R. Harriott, H. Temkin, InGaAs/InP quantum wells with thickness modulation, Appl. Phys. Lett. 65 (7) (1994) 857–859.
[35] Y. Xing, D. Zhao, D. Jiang, Z. Liu, J. Zhu, P. Chen, J. Yang, F. Liang, S. Liu, L. Zhang, Carrier redistribution between two kinds of localized states in the InGaN/GaN quantum wells studied by photoluminescence, Nanoscale Res. Lett. 14 (1) (2019) 1–8.
[36] I. Fraj, T. Hidouri, F. Saidi, H. Maaref, Carrier localization in In0.21Ga0.79As/GaAs multiple quantum wells: a modified Pässler model for the S-shaped temperature dependence of photoluminescence energy, Superlattice. Microst. 102 (2017) 351–358.
[37] T. Hidouri, S. Nasr, Graphene induced weak carrier localization in InGaN nanorods directly grown on graphene-covered Si, Diam. Relat. Mater. 106 (2020) 107841.
[38] H. Dong, K. Qu, J. Liang, A. Zhang, Z. Jia, W. Jia, B. Xu, X. Liu, G. Li, Y. Wu, Evolution mechanism of InGaN quantum dots and their optical properties, Opt. Mater. 99 (2020) 109554.
[39] J. Treu, M. Speckbacher, K. Saller, S. Morkötter, M. Döblinger, X. Xu, H. Riedl, G. Abstreiter, J.J. Finley, G. Koblmüller, Widely tunable alloy composition and crystal structure in catalyst-free InGaAs nanowire arrays grown by selective area molecular beam epitaxy, Appl. Phys. Lett. 108 (5) (2016), 053110.
[40] A.G. Sarwar, M.R. Siddiqui, M.M. Satter, A. Haque, On the enhancement of the drain current in indium-rich InGaAs surface-channel MOSFETs, IEEE Trans. Electron. Dev. 59 (6) (2012) 1653–1660.
[41] B.R. Bennett, J.A. del Alamo, Optical anisotropy in mismatched InGaAs/InP heterostructures, Appl. Phys. Lett. 58 (25) (1991) 2978–2980.
[42] C.J. Humphreys, Does in form In-rich clusters in InGaN quantum wells? Phil. Mag. 87 (13) (2007) 1971–1982.
[43] N.J. Quitoriano, E.A. Fitzgerald, Relaxed, high-quality InP on GaAs by using InGaAs and InGaP graded buffers to avoid phase separation, J. Appl. Phys. 102 (3) (2007), 033511.
[44] Y. Li, Z. Deng, Z. Ma, L. Wang, H. Jia, W. Wang, Y. Jiang, H. Chen, Visualizing carrier transitions between localization states in a InGaN yellow–green light-emitting-diode structure, J. Appl. Phys. 126 (9) (2019), 095705.
[45] D.S. Arteev, A.V. Sakharov, A.E. Nikolaev, W.V. Lundin, A.F. Tsatsulnikov, Temperature-dependent luminescent properties of dual-wavelength InGaN LEDs, J. Lumin. 234 (2021) 117957.
[46] Y. Maidaniuk, R. Kumar, Y.I. Mazur, A.V. Kuchuk, M. Benamara, P.M. Lytvyn, G. J. Salamo, Optical gain and absorption of 1.55μmInAs quantum dash lasers on silicon substrate, *Appl. Phys. Lett.* 11***8*** (6) (2021), 062104.
[47] I. Fraj, T. Hidouri, F. Saidi, L. Bouzaiene, L. Sfaxi, H. Maaref, Effect of carriers localized in clusters on optical properties of In0.21Ga0.79As/GaAs multiple quantum wells, Curr. Appl. Phys. 17 (1) (2017) 1–5.